Simplified stochastic soil-moisture models: a look at infiltration

J. R. Rigby, A. Porporato

Hydrol. Earth Syst. Sci., 10, 861–871, 2006
www.hydrol-earth-syst-sci.net/10/861/2006/

Hydrology and Earth System Sciences

Simplified stochastic soil-moisture models: a look at infiltration

J. R. Rigby and A. Porporato

Department of Civil and Environmental Engineering, Duke University, Durham NC, USA

Received: 20 April 2006 – Published in Hydrol. Earth Syst. Sci. Discuss.: 10 July 2006
Revised: 12 October 2006 – Accepted: 8 November 2006 – Published: 16 November 2006

Abstract. A simplified, vertically-averaged model of soil moisture interpreted at the daily time scale and forced by a stochastic process of instantaneous rainfall events is compared with a vertically-averaged model which uses a non-overlapping rectangular pulse rainfall model and a more physically based description of infiltration. The models are compared with respect to the importance of short time-scale (intra-storm) variable infiltration in determining the probabilistic structure of soil-moisture dynamics at the daily time-scale. Differences in approach to infiltration modelling show only minor effects on the probabilistic structure of soil-moisture dynamics as simulated in the two models. The partitioning of losses during a single rainfall event are examined closely and the conditions under which surface-controlled runoff is significant, as a proportion of total losses, are delineated.

1 Introduction

As both a reservoir and a regulator of water movement in the soil-plant-atmosphere continuum, the soil is an enormously rich and complicated domain for hydrologic enquiry. In ecosystems where water is the limiting resource, understanding the dynamics and variability of soil water is essential not only for understanding the cycling of water, but also for understanding ecosystem dynamics, such as patterns of vegetation form, adaptation, and distribution (both spatially and temporally) (Rodriguez-Iturbe and Porporato, 2004). However, these are complex, nonlinear systems making mathematical analysis of the dynamics difficult. Development of simplified soil-moisture models (e.g., Eagleson, 1978c; Milly, 1993; Kim et al., 1996; Rodriguez-Iturbe et al., 1999; Laio et al., 2001; Porporato et al., 2004; Rodriguez-Iturbe and Porporato, 2004; Daly and Porporato, 2006) is therefore an important step in assembling the analytical tools necessary to unravel the intertwined dynamics of ecosystems and the hydrologic cycle. The aim of developing such models is to balance the faithful representation of physical dynamics (e.g., nonlinearities of infiltration and plant dynamics) against the mathematical simplicity that may allow analytical solutions. These solutions in turn provide insight into the relationships between component processes in determining the character of soil water dynamics.

One of the many tasks in developing simplified models of soil moisture is determining how to represent the partitioning of rainfall into runoff and infiltration. Two mechanisms are commonly associated with runoff: that of subsurface control or saturation deficit, and surface control (often associated with Horton). While the distinction is somewhat artificial, it is useful for describing approximate models of infiltration which require an imposed discontinuity in the infiltration curve at saturation (s=1) to avoid supersaturating the soil. By surface-controlled runoff here we mean runoff generated due to an explicitly time dependent soil infiltrability. By subsurface control we simply mean that, for time resolved events, at saturation the infiltrability is instantaneously reduced to the saturated conductivity or that, for instantaneous events, the infiltrated depth cannot exceed the saturation deficit. In simplified models it is often convenient to ignore surface-controlled runoff in favor of the saturation deficit approach given its simple implementation (Rodriguez-Iturbe et al., 1999; Rodriguez-Iturbe and Porporato, 2004). In this paper we examine the relationship between models treating runoff solely from the saturation deficit approach in favor of analytical (probabilistic) solutions and models which take into account surface-controlled runoff at some analytical cost.

To make such a comparison we have selected two models (each with some modifications for the purposes of this investigation) of soil moisture at a point which broadly illustrate the differing treatments of infiltration while otherwise remaining similar in structure. The first model is that of

Correspondence to: J. R. Rigby
(jrrigby@duke.edu)

Published by Copernicus GmbH on behalf of the European Geosciences Union.

Rodriguez-Iturbe et al. (1999) (see also Milly, 1993; Laio et al., 2001; Porporato et al., 2004) which models soil moisture at the daily time-scale using instantaneous rainfall events and ignoring surface-controlled runoff. We will hereafter refer to this model as the Instantaneous Event Model (IEM). The second model is derived from those of Eagleson (1978b,c) and Kim et al. (1996) which take into account rainfall duration/intensity and the associated possibility of surface-controlled runoff. This model will be referred to as the Finite Duration Event Model (FDEM). Both the IEM and the FDEM treat soil-moisture content averaged vertically over the root zone (i.e., instantaneous vertical redistribution). For a comparison of vertically lumped versus distributed models see Guswa et al. (2002).

The fundamental differences between the two models are in the representation of rainfall and infiltration. For models using the saturation deficit approach it is not necessary (at the daily time scale) to resolve the dynamics of soil moisture during the rainfall event (since only the initial soil saturation deficit and the rainfall depth determine the infiltration response). In such models an instantaneous pulse of rainfall containing a finite depth may then be used as a model for rain events. Alternatively, in order to resolve surface-controlled runoff the model must also ascribe an intensity to the rainfall event in order to determine the infiltration. This amounts to assigning a (stochastic) duration to each rainfall event and then defining a function which transforms a given rainfall depth and duration into an infiltrated depth. In the absence of an analytical solution for this transformation, storm events must be resolved numerically. Otherwise, at the daily time scale a new probability density of jumps in soil moisture could be derived from the known distribution of rainfall depths. For the second model in this paper we follow the approach of Eagleson (1978c) and Kim et al. (1996) in using Philip's (1957) infiltration solution modified by the time compression approximation (e.g., Smith, 2002) as the basis for this function. The two models for comparison differ then only in accounting losses during storm events. As the stochastic forcing is generally the factor determining analytical tractability of the problem, it is of particular interest to understand what is gained from the added complexity of resolving storm duration and whether modifications of the instantaneous storm models are available which might retain the possibility of analytical solutions while improving the accuracy of the model.

2 Description of models

The basic structure of vertically-averaged models of soil moisture at the daily time-scale is that of a stochastic differential equation describing the rate of change in soil moisture as the sum of inputs and losses associated with the active soil layer. The balance equation is then given by

$$nZ_r \frac{ds}{dt} = \phi(R_t) - ET - L, \tag{1}$$

where n is the soil porosity, Z_r is the soil rooting depth (active layer), s is the vertically averaged relative soil-moisture content, ϕ is an infiltration function, R_t represents a stochastic rainfall process, ET is the rate of evapotranspiration, and L represents the losses to deep percolation. Runoff (and infiltration) mechanisms are contained in ϕ which may be a nonlinear function including thresholds (e.g., at s=1).

In this section we describe two models that may be expressed in the manner of Eq. (1): the IEM, which models rainfall as a marked Poisson process, and the FDEM, which models rainfall using random rectangular pulses. As the models differ primarily in the processes at work during a rainfall event, we will divide the description of the models into "during storm" and "between storm" components.

Between storm events both models evolve according to the same equation representing losses due to evapotranspiration and percolation, following Kim et al. (1996),

$$nZ_r \frac{ds}{dt} = -(k_s s^{c+1} + E_{\max} s), \tag{2}$$

where k_s is the saturated hydraulic conductivity, c=2(1+m)/m where m is the exponent in the Brooks and Corey (1966) water retention relation, and $E_{\max}$ is the potential evapotranspiration. Here percolation is modelled after the Brooks and Corey (1966) relation for unsaturated conductivity. Evapotranspiration is assumed to decrease linearly with soil moisture from a maximum at saturation, $E_{\max}$, following Kim et al. (1996). While in general the evapotranspiration tends to be a nonlinear function of soil moisture (Rodriguez-Iturbe et al., 1999), the linear evapotranspiration losses have been found to be reasonable for a broad range of soil-moisture values (see Porporato et al., 2004, and references therein). For the purposes of this paper, the loss function given in Eq. (2) is adopted for both the instantaneous and finite duration models.

While the models are identical in their representation of soil moisture between storms, the models differ significantly in their treatments during a rainfall event. In the following sections we describe the particulars of the stochastic rainfall process and soil-moisture accounting in each model.

2.1 Instantaneous Event Model (IEM)

2.1.1 Rainfall

Since both the occurrence and amount of rainfall can be considered to be stochastic, the occurrence of rainfall is here idealized as a series of point events in continuous time, arising according to a Poisson process of rate λ, each carrying a random amount of rainfall extracted from a given distribution. The temporal structure within each rain event is ignored

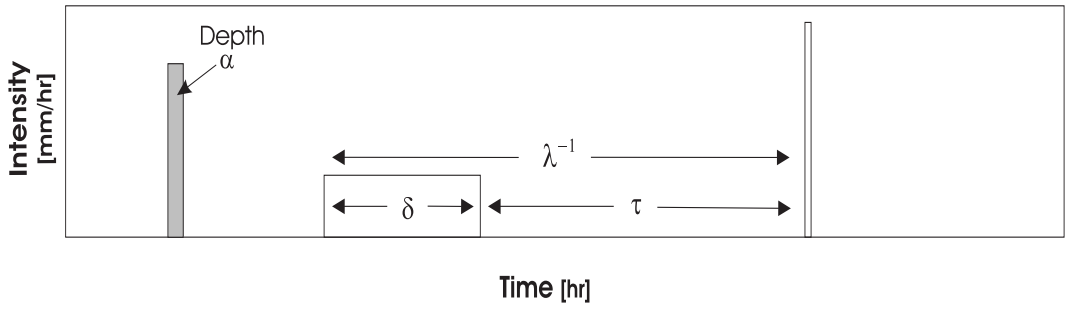

Fig. 1. Summary of the stochastic rainfall model used by Eagleson (1978c). The frequency, λ, for the corresponding marked Poisson process, used in the IEM, is also shown. The mean rainfall depth α represents the mean area of the rectangular pulses.

and the marked Poisson process representing precipitation is physically interpreted at a daily time-scale, where the pulses of rainfall corresponding to daily precipitation are assumed to be concentrated at an instant in time.

With these assumptions, the distribution of the times between precipitation events is exponential with mean $1/\lambda$ (e.g., Cox and Miller, 1965). Furthermore, the depth of rainfall events is assumed to be an independent random variable D, described by an exponential probability distribution where α is the mean depth of rainfall events.

Both the Poisson process and the exponential distribution are of common use in simplified models of rainfall at the daily time scale. The exponential distribution fits well daily rainfall data and, at the same time, allows analytical tractability (Benjamin and Cornell, 1970; Eagleson, 1978a,c). The values of α and λ are assumed to be time-invariant quantities, representative of a typical growing season.

2.1.2 Infiltration

In the IEM the Poisson rainfall process creates an instantaneous jump in soil moisture such that the infiltration depth, I_D, is assumed equal to the minimum value between the soil saturation deficit and the depth of the rainfall event, i.e.,

$$I_D = \min\left[nZ_r(1-s_0), D\right], \tag{3}$$

where s_0 is the relative soil moisture at the beginning of the event and D represents the total depth of the rainfall event (Rodriguez-Iturbe et al., 1999; Rodriguez-Iturbe and Porporato, 2004). For later comparison with the FDEM a normalized infiltration function, $y(\widetilde{D}, s_0)=I_D/nZ_r$, representing the net increase in relative soil moisture due to a rainfall event of dimensionless depth, $\widetilde{D}=D/nZ_r$, can be defined as

$$y(\widetilde{D}, s_0) = \begin{cases} \widetilde{D}, & 0 \le \widetilde{D} \le (1-s_0) \\ 1-s_0, & \widetilde{D} > (1-s_0). \end{cases} \tag{4}$$

Any rainfall in excess of $1-s_0$ is attributed to cumulative losses (i.e., the combined effect of runoff and percolation).

2.1.3 Model summary

The IEM is a vertically averaged model of soil moisture interpreted at the daily time-scale, driven by a marked Poisson rainfall process of rate λ with exponentially distributed depths of mean α. The instantaneous jump in soil-moisture state for a particular event is determined completely by the subsurface state, or saturation deficit, and the depth of the rainfall event. Losses between storms are assumed due only to evapotranspiration and percolation. This may be expressed by the stochastic differential equation,

$$nZ_r\frac{ds}{dt} = I_D(R_t, s_0) - (k_s s^{c+1} + E_{\max}s). \tag{5}$$

The stochastic soil-moisture process described by Eq. (5) may be solved analytically under steady state conditions (Rodriguez-Iturbe and Porporato, 2004). The resulting probability distribution is, in this case,

$$p(s) = Cs^{\frac{\lambda}{\eta}-1}e^{-\gamma s}(E_{\max}+k_s s^c)^{-\frac{\lambda}{c\eta}-1}, \tag{6}$$

where $\eta=E_{\max}/nZ_r$ and C is a normalization constant that must be evaluated numerically.

2.2 Finite Duration Event Model (FDEM)

2.2.1 Rainfall

Eagleson (1978c) offered an alternative to the Poisson rainfall process to allow for surface-controlled runoff by modelling rainfall with non-zero storm durations. In contrast to the marked Poisson process, each rainfall event is a rectangular pulse occupying a finite time, with the time between storms distributed exponentially with mean τ. A probability distribution is also assigned to the storm durations as well as to either the intensity or the total depth of rainfall. The remaining distribution may then be derived from the other two. Drawing on data from Massachusetts and California, Eagleson (1978b) found that the durations were fit reasonably well by the exponential distribution (with mean δ, see Fig. 1) and that the event depths fit a two parameter gamma distribution. Eagleson (1978b) then employed a model based on assumed

distributions for the depth and duration of rainfall events. Given that the exponential distribution is a special case of the two parameter gamma distribution, we will use the simpler exponential form in this paper so that the two rainfall models (IEM and FDEM) agree with respect to the distribution of depths. Thus, for our finite duration model, each rainfall event is determined by three random variables (depth, duration, and inter-arrival time), each of which is drawn from an exponential distribution.

Assuming statistical independence between rainfall depth and duration, one may now derive the distribution of rainfall intensities dictated by fixing the distribution of depths and durations as an exponential. The resulting probability density function is

$$f_P(P) = \frac{\alpha\delta}{(\alpha + \delta P)^2} \tag{7}$$

which is the positive part ($P>0$) of a Cauchy distribution. As Eagleson (1978b) found that measured rainfall intensities were modelled well as an exponential distribution, the Cauchy distribution, with power law tails, should overestimate the frequency of intense rain events and the corresponding runoff. Furthermore, while depth and duration are assumed independent variables, sampling from these two distributions for each rainfall event leads to a statistically dependent intensity. The conditional distribution of intensity, P, given the event duration, w, is then, $f_{P|w}(P|w)=\frac{w}{\alpha}e^{-\frac{w}{\alpha}P}$, which shows the negative correlation between intensity and duration. Such negative correlation is consistent with observed rainfall frequency-duration patterns, though the negative correlation here is probably exaggerated due to the simple rainfall model.

2.2.2 Infiltration

To treat infiltration, the FDEM follows Eagleson (1978c) and the improvements of Kim et al. (1996) by employing Philip's (1957) approximate solution (hereafter Philip solution) to Richards' equation combined with the time compression approximation.

Assuming a constant hydraulic head at the soil surface with an initially uniform (semi-infinite) vertical soil-moisture profile, Philip (1957) obtained a series solution to Richards' equation. In its truncated form, the approximate solution states that the infiltration rate, $i(t)$, decreases in time as

$$i(t) = 1/2S(s_0)t^{-1/2} + ak_s \tag{8}$$

where t is the time since the inception of the rainfall event, and $S(s_0)$ represents the soil sorptivity and may be expressed as

$$S(s_0) = \left(\frac{2n(1-s_0)\psi_s}{1+3m}(s_0^{(1+3m)/m} - 1)\right)^{1/2} k_s^{1/2} \tag{9}$$

where ψ_s is the Brooks and Corey (1966) air entry pressure (Smith and Parlange, 1978). The constant a in Eq. (8) which depends on unsaturated hydraulic conductivity near saturation (see Parlange et al., 1982) is here taken to be unity for consistency with percolation losses at very long event durations (see Sect. 2.2.3).

For small t, according to the Philip solution, the potential rate of infiltration of the soil will exceed the precipitation rate. With these assumptions the infiltration rate curve would then be equal to the precipitation rate, P, up to time t_e when the Philip potential infiltration rate equals the precipitation rate, after which ponding should begin. Thus,

$$i(t) = \begin{cases} P, & 0 \le t \le t_e \\ 1/2S(s_0)t^{-1/2} + k_s, & t > t_e \end{cases} \tag{10}$$

(see Fig. 1). Setting Eq. (8) equal to P and solving for time yields,

$$t_e = \frac{S(s_0)^2}{4(P-k_s)^2}, \qquad P > k_s. \tag{11}$$

However, initially, the boundary condition is that of constant flux (equal to P) rather than the constant head assumed in the Philip solution. The result is that the time to ponding, t_p, is not generally equal to t_e and is found to be somewhat larger. Liu et al. (1998) provide a nice description of the exact solution for one dimensional linearized infiltration. As an approximate correction for the difference between the exact infiltration solution and the Philip solution, according to the time-compression approximation (TCA) (also termed the Infiltrability-Depth Approximation, see Smith, 2002, for detailed discussion), cumulative infiltration may be used as a surrogate for time (Sherman, 1943; Liu et al., 1998). Accordingly, one assumes that at time t_p the cumulative infiltration under the constant flux is equal to the cumulative infiltration under the Philip curve up to time t_e. The time to ponding, $t_p=t_e+t_c$ where t_c is the time of compression representing the difference between ponding in the Philip solution and the actual time to ponding, is then defined by

$$\int_0^{t_p} P dt = \int_0^{t_e} i(t) dt \tag{12}$$

where $i(t)$ is the Philip solution from Eq. (8). From this definition it follows that

$$t_p = \begin{cases} \frac{S(s_0)^2(2P-k_s)}{4P(P-k_s)^2}, & P > k_s \\ \infty, & P \le k_s\ . \end{cases} \tag{13}$$

Making the added assumption that for $t \ge t_p$ the infiltration rate follows the Philip curve, the infiltration rate from Eq. (10) becomes

$$i(t) = \begin{cases} P, & 0 \le t \le t_p \\ 1/2S(s_0)(t-t_c)^{-1/2} + k_s, & t > t_p. \end{cases} \tag{14}$$

Furthermore, we can express the cumulative infiltration depth (i.e., the cumulative depth of infiltrated rainfall)

analytically by integrating Eq. (14)

$$I_D(t) = \begin{cases} Pt, & 0 \le t \le t_p \\ Pt_p + S(s_0)\left((t-t_c)^{1/2} - t_e^{1/2}\right) & \\ \quad +k_s(t-t_p). & t > t_p \end{cases} \quad (15)$$

From Eq. (15) one may now derive the normalized cumulative infiltration $y(\widetilde{D}, s_0)$ in analogy with that for the IEM, Eq. (4), as a function of the non-dimensional rainfall depth by dividing Eq. (15) by nZ_r, substituting D/P for t, and then non-dimensionalizing the precipitation rate by $\widetilde{P}=P/k_s$. The result is the somewhat complicated expression,

$$y(\widetilde{D}, \widetilde{P}, s_0) = \begin{cases} \widetilde{D}, 0 \le \widetilde{D} \le \frac{k_s}{nZ_r}\widetilde{P}t_p \\ \frac{k_s}{nZ_r}\widetilde{P}t_p + \\ \quad \frac{S(s_0)}{nZ_r}\left(\left(\frac{nZ_r\widetilde{D}}{k_s\widetilde{P}} - t_c\right)^{1/2} - t_e^{1/2}\right) + \\ \quad\quad k_s\left(\frac{nZ_r\widetilde{D}}{k_s\widetilde{P}} - t_p\right), \widetilde{D} > \frac{k_s}{nZ_r}\widetilde{P}t_p \end{cases} \quad (16)$$

where t_p, t_e, and t_c are all functions of both s_0 and $\widetilde{P}$. Notice that since Philip's solution assumes a semi-infinite domain, the cumulative infiltration is potentially infinite.

2.2.3 Losses during rainfall

The model of infiltration described in the previous section only accounts for the cumulative infiltration across the soil surface and does not provide explicitly a method for determining the soil-moisture content of an active layer of soil. In order to model the change in mean soil moisture content in the upper soil layer (of depth Z_r) it is necessary to keep an account of the flux of water across the lower bound of this layer (i.e., percolation) during the rainfall event.

In the Kim et al. (1996) model, however, losses were only included during the inter-storm periods. One consequence is shown clearly by comparing the time to soil saturation (given the linear increase in relative soil moisture during the period prior to ponding) with the calculated time to ponding derived from the time compression approximation. Combining Eqs. (9) and (13),

$$t_p = \left(\frac{nZ_r(1-s_0)}{P}\right)\left(\frac{\psi_s k_s (s_0^{(1+3m)/m} - 1)(2P - k_s)}{2Z_r(1+3m)(P-k_s)^2}\right), \quad (17)$$

from which it is clear that the first bracketed term represents the time to saturation if ponding does not occur, and thus that the second bracketed term must be less than or equal to unity in order for ponding to occur before the soil is saturated (a reasonable physical requirement). This condition is, in fact, not met identically.

Figure 2 illustrates the domain in which ponding occurs before saturation. Kim et al. (1996) account for this possibility by including it as part of "infiltration excess." So, while the time to ponding may in some cases violate physical sense,

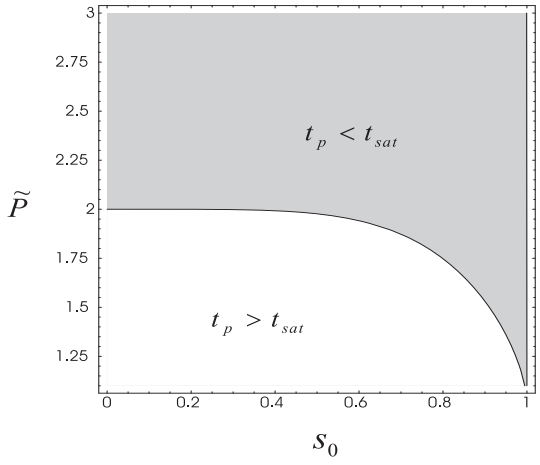

Fig. 2. Plot showing the domain in which the Kim et al. (1996) model by ignoring percolation during storm events produces the unphysical result that the time to ponding is greater than the time to saturation. Shown for n=0.4, Z_r=300 mm, s_0=0.5, k_s=200 mm day^{-1}, ψ_s=−500 mm, m=0.5.

it presents no problem for simulation due to the bound imposed at s=1.

In order to avoid this unphysical result, the FDEM first incorporates percolation during storm events in the same form as Eq. (2). Following Kim et al. (1996) we assume that evapotranspiration is negligible during storm events. One then has $-k_s s^{c+1}$, which is simply the loss for periods between storms, Eq. (2), without the evapotranspiration term. However, taking into account leakage during the storm in this manner does not solve the problem satisfactorily. While the percolation losses will strictly balance with Eq. (14) for very long durations, for finite times the infiltration term involving the sorptivity will still produce a supersaturation. This is due to the approximate nature of both the infiltration and the loss equations. In reality, soil moisture should asymptotically, and monotonically, approach saturation during a precipitation event of constant intensity. Thus, to prevent the supersaturation we further impose a bound at s=1 which, however, produces a discontinuity in the $s(t)$ curve which is strictly an artifact of the model. The difference between the soil-moisture curve without the bound at s=1 and that with the bound represents the model's error in properly allocating moisture to runoff, storage, or leakage. Under our distinctions between runoff mechanisms it is therefore attributed to subsurface-controlled runoff. In the FDEM this term is typically small compared with the other losses.

2.2.4 Model summary

Following Eagleson (1978b,c) and Kim et al. (1996) the FDEM is a physically-based model of vertically averaged soil moisture at the daily time scale which incorporates Philip's (1957) infiltration solution coupled with the

Table 1. Table of parameter values used in simulation of soil-moisture and rainfall processes.

Name	Units	Value
ψ_s	mm	-500
k_s	mm day^{-1}	50, 200, 2000
m	$-$	0.5
Z_r	mm	300, 600
τ	h	74
δ	h	4, 6
λ	day^{-1}	0.15, 0.3
α	mm	12
$E_{\max}$	mm day^{-1}	3

time compression approximation and the Brooks and Corey (1966) model for percolation. The FDEM uses a non-overlapping, rectangular pulse model for rainfall for which the depths and durations are drawn from corresponding exponential distributions with means α and δ. The mean inter-arrival time, τ, is then chosen to be consistent with that of the IEM, $\lambda=(\tau+\delta)^{-1}$.

The evolution of soil moisture during storm events is described by the equation

$$nZ_r\frac{ds}{dt}=\begin{cases} i(P,s_0,t)-k_s s^{c+1}, & s<1 \\ 0, & s=1 \end{cases} \tag{18}$$

where $i(P,s_0,t)$ is the time dependent infiltration rate (given by Eq. 14 for a single rainfall event) and P is the rainfall intensity. In the FDEM, as with the IEM, a bound is imposed at $s=1$. Between storm events the model evolves according to Eq. (2). The steady-state probabilistic structure of this process is not known analytically and is thus determined by numerical simulation.

3 Model comparisons

A combination of numerical simulations and analytic solutions were used to compare the two models. Analytic solutions exist for Philip's infiltration with time compression approximation, as well as for the probability density of the full soil-moisture process defined in the IEM, Eq. (6).

Figure 4 illustrates the correspondence between the IEM and the FDEM for a simulation period of 100 days. The traces are almost identical with a notable exception near the beginning of the series where an extremely intense storm occurred. As seen to the right of the time series, the simulated probability distribution of relative soil moisture generated with the FDEM agrees well with the analytical solution to the IEM.

The net effect of the differences in infiltration modelling between the IEM and FDEM is illustrated in Figs. 5 and 6 which show the probability distributions of soil moisture for the two models. The four plots in Fig. 5 represent independent simulations between which the soil depth, mean rainfall frequency, and mean rainfall duration were varied. As one would expect, the FDEM simulation shows the greatest departure from the IEM when the soil is deep and rainfall is infrequent. Under these conditions the mean soil-moisture state is relatively dry leading to a high mean saturation deficit, while rainfall intensities are also high, leading to significant losses to runoff for the FDEM. However, even in these cases the correspondence between the two is very good. Figure 6 shows similar results for two different saturated conductivity values representing two orders of magnitude difference. Unsurprisingly, the deep clay soil shows the greatest discrepancy. Still the difference appears to be primarily in the position and less in the shape of the distribution.

Given the correspondence between the two models evident from Figs. 4 and 5, it is worth taking a closer look at the relative importance of runoff and percolation in determining the change in soil moisture state due to a single event. Figure 7 illustrates the relationships between the models as they account for the partitioning of a rainfall event into constituent depths. The plot on the left shows the simple partitioning of the IEM into the depth contributing to a change in soil moisture and cumulative losses for a storm event as a function of rainfall depth for a given rainfall intensity and initial soil moisture state. The plot on the right of Fig. 7 gives a detailed account of the partitioning in the FDEM: The diagonal line of unit slope represents the dimensionless depth of water input to the system (equal to the event depth normalized by nZ_r). The curve just below this represents the infiltration model of Kim et al. (1996) comprising the Philip (1957) infiltration solution and the time compression approximation. The difference between the two upper curves is that portion of the total depth which is lost to surface-controlled runoff. The next lowest curve in the diagram is that of the FDEM without the bound at $s=1$. The difference between the Kim et al. (1996) and FDEM curves is the effective portion of rainfall contributing to percolation. The bold curve represents the FDEM taking into account the bound at at $s=1$ and represents the portion of a rainfall event that is stored in the rooting zone (i.e., the change in soil-moisture state). The difference between the FDEM curve without the bound at $s=1$ and this bold curve is then a loss associated with the model error due to the approximation of infiltration and percolation functions and is here termed subsurface-controlled runoff.

From the point of view of simplified soil-moisture models one should notice that for all event depths the dominant loss during rainfall events is percolation (Fig. 7, shown for $\widetilde{P}=2$). The character changes significantly for $\widetilde{P}>2.5$ (not shown) as runoff plays a strongly increasing role. Secondly, the diagram in Fig. 7 may be somewhat misleading with respect to the values of $\widetilde{D}$ one may expect to encounter. A typical mean event depth, $\alpha=12$ mm (used for the simulations in this paper), yields a mean value of $\widetilde{D}$ between 0.1 and 0.2 (depending on Z_r). In fact, $\widetilde{D}<0.3$ for 95% of the rainfall

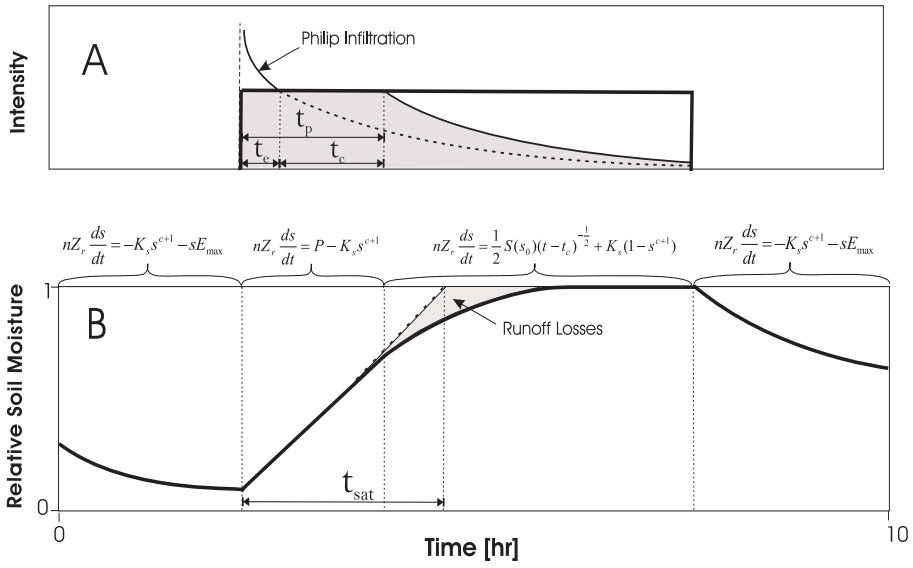

Fig. 3. Summary of the FDEM incorporating Philip's infiltration solution with the time compression approximation for a rectangular rainfall pulse. The differential equations governing the soil-moisture process are shown above the corresponding time periods.

events drawn from this exponential distribution. From the diagram, at $\widetilde{D}$=0.3 the losses are almost entirely due to percolation. For larger rainfall intensities the proportion of losses due to runoff will increase, though for sites with moderate clay content the average rainfall intensity is unlikely to be much greater than that shown, particularly for longer durations. Figure 8 shows the fraction of total losses (runoff and percolation) due to surface-controlled runoff in the FDEM. The multiple curves can be interpreted as either increasing clay content for a given intensity or increasing precipitation intensity for a given soil. For large depth events (long duration) the fraction of losses due to runoff approach (approximately) $L_R/L_{\text{tot}}=1-1/\widetilde{P}$. The relation is only approximate because of the model error which produces the small subsurface-controlled runoff term. Notice that for ponding to occur at such small event depths ($D\approx$25 mm) for s_0 near the mode of the distribution, the intensity must be at least 3.5 times the saturated hydraulic conductivity.

While Fig. 7 illustrates the deterministic partitioning of a rainfall event into infiltration, runoff and percolation, this reveals little of the behavior of the two models as the parameters s_0 and $\widetilde{P}$ vary (stochastically) during a growing season. Figure 9 shows how the change in relative soil-moisture state, y, due to a single rainfall event varies with rainfall intensity and initial soil-moisture state in the two models. Notice that the change in soil moisture, especially for small values of $\widetilde{D}$, is strongly controlled by s_0.

Given the one-to-one relation between event depth and change in soil-moisture state (for given values of s_0 and P) represented by these curves along with the distribution of event depths, we may derive the probability distribution of change in soil-moisture state simply by transformation of

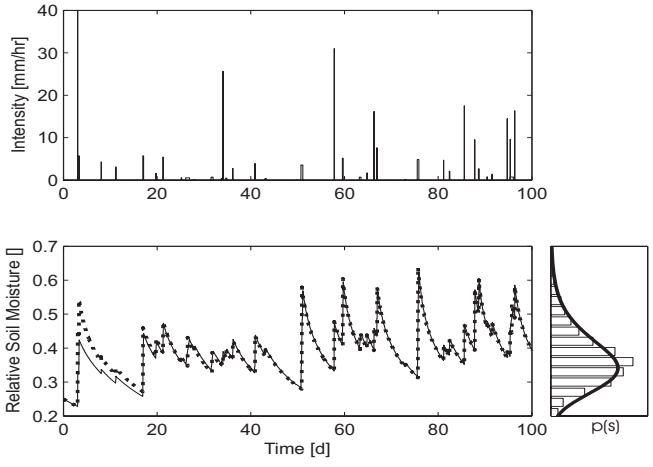

Fig. 4. Comparison of FDEM (solid line) and IEM (dotted line) soil-moisture models over one hundred days. The stochastic rainfall series of rectangular pulses is shown above. To the right is shown the simulated p.d.f. of the FDEM model (bars) with the analytic p.d.f. of the IEM model.

variables. The result of the transformation, performed numerically, is shown in Fig. 10. Comparison of the two plots in Fig. 10 again supports the observation that the change in soil moisture due to a storm event is significantly more sensitive to initial soil-moisture state than to rainfall intensity. For s_0=0.8 the IEM significantly overestimates the probability of saturation (represented by the Dirac delta function at $\widetilde{D}=1-s_0$). The shape of the distributions from the FDEM as s_0 increases may be somewhat counterintuitive. Taking the s_0=0.8 case as an example, the shape can be understood by

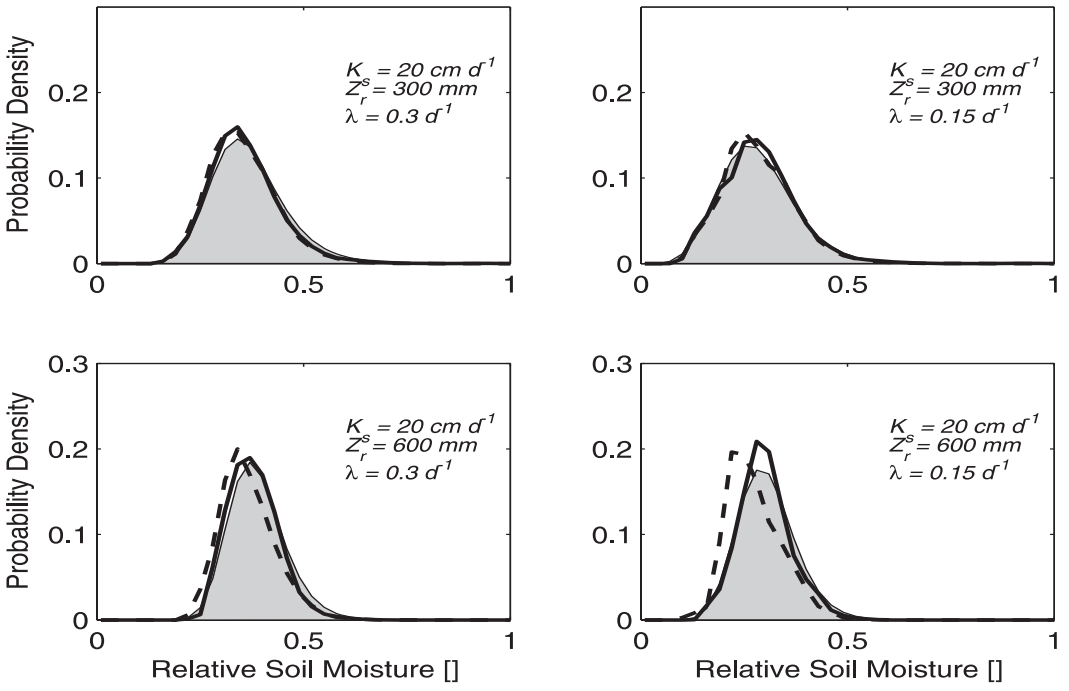

Fig. 5. Comparison of simulated FDEM (lines) and analytic IEM (shaded area) probability distributions for soil moisture. The four plots show varying soil depth and rainfall arrival rates. The two lines on each plot are for mean rainfall durations of 4 (solid) and 6 (dotted) hours. The plots on the left correspond to an index of dryness ($\lambda\alpha/E_{\max}$) of 1.2 while those on the right have an index of 0.6.

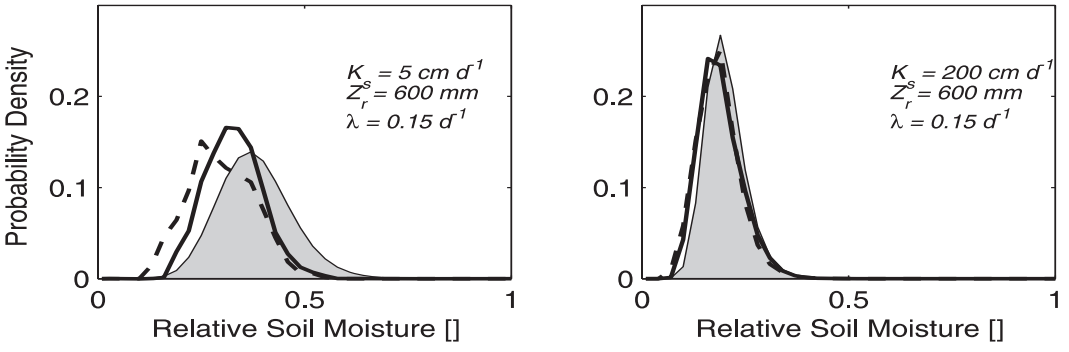

Fig. 6. Comparison of simulated FDEM (lines) and analytic IEM (shaded area) probability distributions for soil moisture. The two plots show the effect of soil saturated hydraulic conductivity on the correspondence between pdf's of soil moisture according to the IEM and FDEM. The two lines on each plot are for mean rainfall durations of 4 (solid) and 6 (dotted) hours.

referring back to the diagram in Fig. 3. For $t<t_p$ the change of variables is just a re-scaling of the exponential curve. For durations (where storm duration and time are used here interchangeably) longer than t_p the duration necessary to saturate the soil is significantly longer for the FDEM. In effect, a larger domain of event depths contributes to a smaller range of changes in soil moisture, which results in a redistribution of probability from the atom at saturation for the IEM to values of $y<1-s_0$. For s_0=0.8 the IEM has an atom of probability (exceedence probability for $\widetilde{D}=1-s_0$) of approximately 0.14, while that for the FDEM model has an atom of only about 0.02.

Examination of the distribution of net infiltration, y, as s_0 and $\widetilde{P}$ vary suggests no particularly straightforward method to improve the IEM with respect to losses during rainfall events. One possible correction is introduce another element of state dependence into the jump distribution. Whereas the IEM currently uses a jump distribution that is an exponential truncated at $y=1-s_0$ with mean $\gamma=\alpha/nZ_r$, one might define a state dependent mean which maps an exponential probability distribution with the same atom of probability at $1-s_0$ as the FDEM distribution onto each value of s_0. Such an approach is the subject of future research and may still yield to analytical solution. This sort of correction is most likely

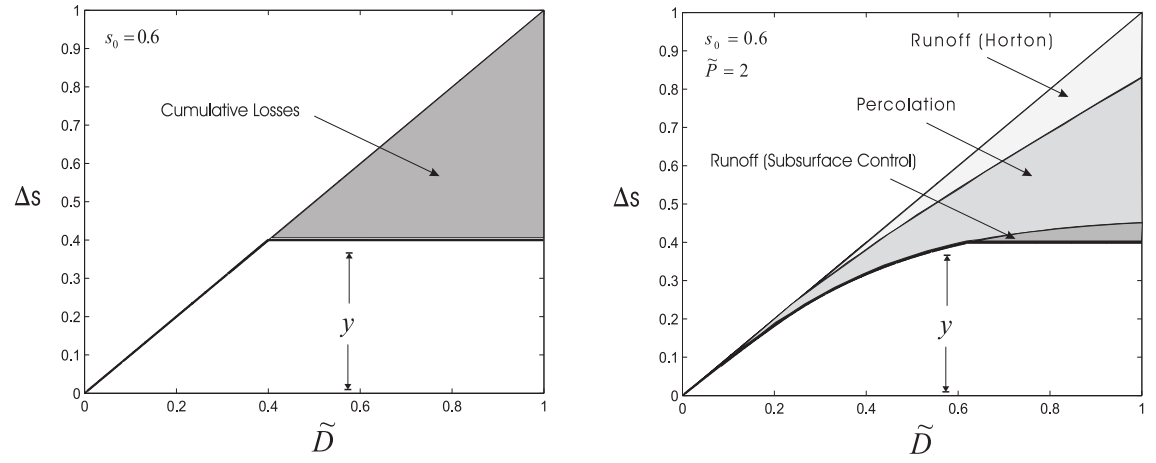

Fig. 7. Rainfall partitioning during a storm event for the IEM (left) and the FDEM (right). The vertical axis represents the rainfall depth transformed by processes of infiltration and percolation. The normalized curves in the FDEM plot are, from highest to lowest: depth of rainfall event (slope = unity), infiltrated depth according to Kim et al. (1996), infiltrated depth minus percolation according to FDEM without bound at s=1, and the bold line represents the actual change in soil-moisture state as a function of rainfall depth according to the FDEM with the bound at s=1.

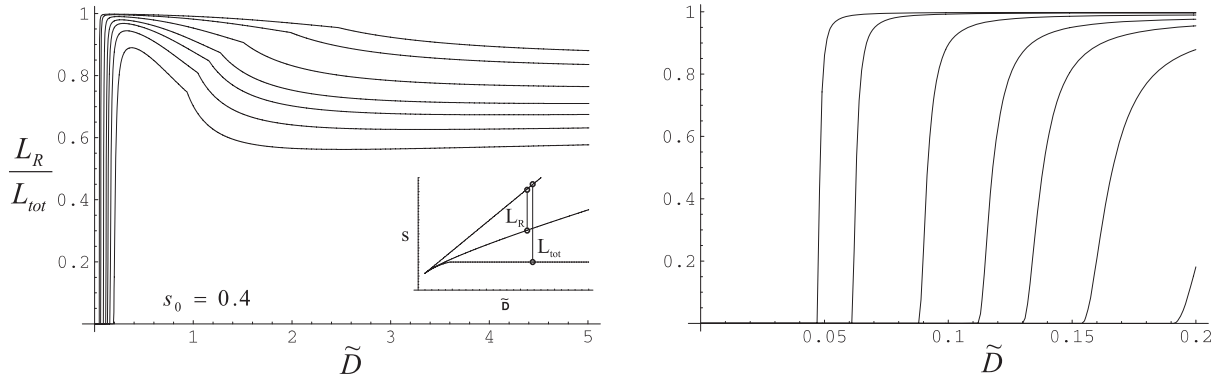

Fig. 8. Fraction of losses attributed to runoff as a function of total rainfall depth for both **(a)** very large depths and **(b)** typical rainfall depths. The curves represent different precipitation intensities increasing from the right: 3.5, 4, 4.5, 5, 6, 8, and 10, respectively.

to be of use in wetter climates where the probability of high soil-moisture values is significant. Otherwise, as can be seen in Fig. 10, the effect of corrections will probably be of little value.

4 Conclusions

We have presented two models to compare the importance of resolving variable infiltration during storm events in capturing the dominant characteristics of soil-moisture dynamics. The first is a model of vertically averaged soil moisture forced by a marked Poisson arrival process. The second model is rooted in the treatment by Eagleson (1978c) and Kim et al. (1996) with a physically based description of infiltration which was further modified in this paper to include percolation losses.

In resolving both runoff and percolation, we have shown evidence that accounting for fractional loss to leakage during a storm event is probably of equal or more concern for improving the accuracy of simplified models than is runoff, particularly for events of lower intensity and longer duration. It is worth noting once more the significant difference between the IEM and the model of Kim et al. (1996) in which losses during the storm event were neglected. The latter model is similar to the IEM except that it accounts for variable infiltration during the rainfall event. However, neglecting the losses to percolation (particularly for long durations) is a significant weakness for the Kim et al. (1996) model. Since in the IEM events are instantaneous, percolation continues essentially uninterrupted. The IEM error is thus concentrated at an instant in time and is then damped quickly by the strongly nonlinear character of percolation, while the Kim et al. (1996) model spreads the error over the duration of the

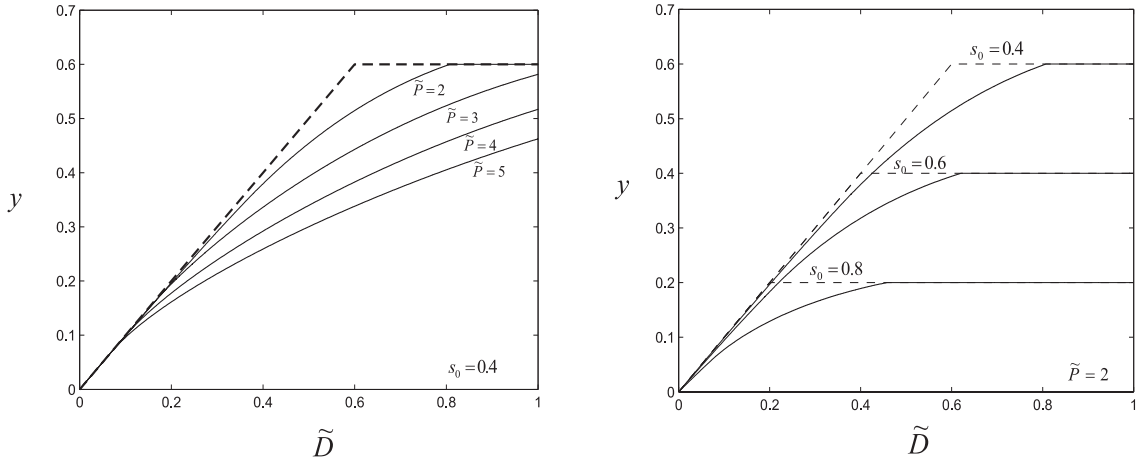

Fig. 9. Change in soil moisture, $y{=}\Delta s$, representing normalized net infiltration, for different values of $\widetilde{P}$ (left) and s_0 (right) for both the IEM and FDEM models. The dotted lines represent the IEM model.

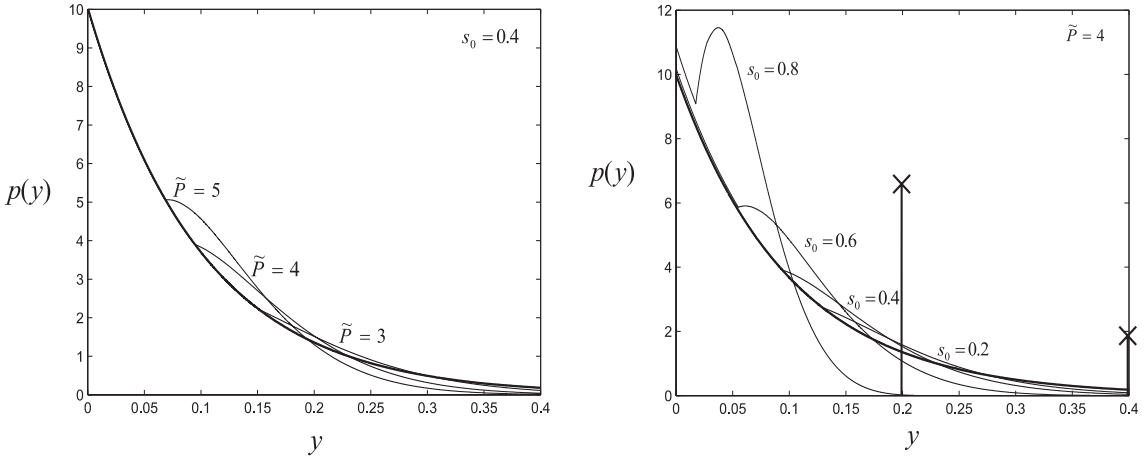

Fig. 10. Derived distributions of the normalized net infiltration for both the IEM and FDEM. Note that the IEM distribution (bold) is a truncated exponential with an atom of probability at $\widetilde{D}{=}1{-}s_0$ represented by the corresponding Dirac delta functions.

event. For longer rainfall durations, therefore, the Kim et al. (1996) model may be expected to overestimate infiltration to a greater extent than the IEM. In such cases the gains of representing temporally extended rainfall events with variable infiltration are outweighed by the error of neglecting percolation.

The highly simplified IEM performs well against more complex, physically-based models such as the FDEM (Fig. 4) in reproducing the probabilistic structure of soil-moisture dynamics (Fig. 5). As expected, the most significant difference between the models occurs under conditions of intense rainfall over short duration, in which case the IEM will consistently overestimate infiltration. However, Fig. 6 suggests that the primary difference in the probability density is one of location and not shape. Our analysis has been conservative with respect to the frequency of intense rainfall, as the use of Eq. (7) likely overestimates its frequency, thus likely exaggerating the importance of runoff in simulations. Also, while the IEM used here incorporates a very simple mechanism for losses during storm events, the model described by Eq. (5) retains a significant amount of flexibility through the definition of the I_D function. We find, however, that even in this conservative analysis the IEM reproduces well the probabilistic structure of soil-moisture dynamics.

Acknowledgements. The authors would like to thank C. Hinz and M. Sivapalan for their kind invitation to write this paper and organizing the Sir Mark Oliphant Conference: International Frontiers of Science and Technology Thresholds and Pattern Dynamics, University of Western Australia. This research was supported in part by the Office of Science, Biological and Environmental Research Program (BER), U.S. Department of Energy, through the Great Plains Regional Center of the National Institute for Global Environmental Change (NIGEC) under Cooperative Agreement No. DE-FC02-03ER63613, and in part by the Forest-Atmosphere

Carbon Transfer and Storage (FACT-1), funded by the U.S. Department of Energy. We also thank T. Ellis (CSIRO) for stimulating discussions. We would like also to thank F. Laio and S. Manfreda for helpful comments and suggestions.

Edited by: G. Hancock

References

Benjamin, J. R. and Cornell, C. A.: Probability, Statistics and Decision for Civil Engineers, New York, McGraw-Hill, 1970.

Brooks, R. H. and Corey, A. T.: Properties of porous media affecting fluid flow, Journal of Irrigation and Drainage ASCE, 92(IR2), 61–88, 1966.

Cox, D. R. and Miller, H. D.: The Theory of Stochastic Processes, London, Methuen, 1965.

Daly, E. and Porporato, A.: Impact of Hydro-Climatic Fluctuations on the Soil Water Balance, Water Resour. Res., 42, W06401, doi:10.1029/2005WR004606, 2006.

Eagleson, P.: Climate, Soil and Vegetation 1. Introduction to water balance dynamics, Water Resour. Res., 14, 705–712, 1978.

Eagleson, P.: Climate, Soil and Vegetation 2. The distribution of annual precipitation derived from observed storm sequences, Water Resour. Res., 14, 713–721, 1978.

Eagleson, P.: Climate, Soil and Vegetation 3. A simplified model of soil moisture movement in the liquid phase, Water Resour. Res., 14, 722–730, 1978.

Guswa, A., Celia, M., and Rodriguez-Iturbe, I.: Models of soil moisture dynamics in ecohydrology: A comparative study, Water Resour. Res., 38(9), 1166–1181, 2002.

Kim, C., Stricker, J., and Torfs, P.: An analytical framework for the water budget of the unsaturated zone, Water Resour. Res., 32, 3475–3484, 1996.

Laio, F., Porporato, A., Ridolfi, L., and Rodriguez-Iturbe, I.: Plants in water-controlled ecosystems: Active role in hydrologie processes and responce to water stress II. Probabilistic soil moisture dynamics, Adv. Water Resour., 24(7), 707–723, 2001.

Liu, M. C., Parlange, J. Y., Sivapalan, M., and Brutsaert, W.: A note on the time compression approximation, Water Resour. Res., 34, 3683–3686, 1998.

Milly, P. C. D.: An analytic solution of the stochastic storage problem applicable to soil water, Water Resour. Res., 29(11), 3755–3758, 1993.

Parlange, J. Y., Lisle, I., Braddock, R. D., and Smith, R. E.: The three parameter infiltration equation, Soil Sci., 133, 337–341, 1982.

Philip, J. R.: The Theory of Infiltration 4. Sorptivity, and algebraic infiltration equations, Soil Sci., 84, 257–264, 1957.

Porporato, A., Daly, E., and Rodriguez-Iturbe, I.: Soil water balance and ecosystem response to climate change, American Naturalist, 164(5), 625–632, 2004.

Rodriguez-Iturbe, I., Porporato, A., Ridolfi, L., Isham, V., and Cox, D.: Probabilistic modelling of water balance at a point: the role of climate, soil and vegetation, Proc. Royal Soc. London A, 455, 3789–3805, 1999.

Rodriguez-Iturbe, I. and Porporato, A.: Ecohydrology of water-controlled ecosystems: Soil moisture and Plant Dynamics, Cambridge, New York, 2004.

Sherman, L. K.: Comparison of F-curves derived by the methods of Sharp and Holtan and of Sherman and Mayer, Eos Transactions AGU, 24, 465–467, 1943.

Smith, R. E. and Parlange, J. Y.: A paremeter-efficient hydrologic infiltration model, Water Resour. Res., 14, 533–538, 1978.

Smith, R.: Infiltration Theory for Hydrologic Applications, AGU, Washington, D.C., 2002.